Modeling the thermal-to-plasma transitions for Cu photoablation

by A. Vertes
R. W. Dreyfus
D. E. Platt

Excimer laser ablation of metals starts as a thermal process in the ~1-J/cm^2 fluence range and makes a rapid transition near 5 J/cm^2 to a highly ionized plume (for 10-ns pulses). The 1–5-J/cm^2 range is of particular interest because it overlaps the irradiance range used to fabricate high-temperature superconductors, diamondlike carbon films, and conducting Cu films. Covered here are analyses aimed at a quantitative evaluation of the transition using a previously described model. The model is based primarily on the thermal (diffusivity and vapor pressure) properties of copper, along with electron heating by inverse bremsstrahlung due to electrons scattering off both neutrals and ions. The analyses provide a good fit and insight into previously obtained laser-induced fluorescence results for Cu^0, Cu$^+$, and Cu$_2$. Also, the surface shadowing and plasma heating beginning in the 5-J/cm^2 (500-MW/cm^2) region are clearly illustrated.

Introduction

Laser vaporization of surfaces is viewed as a combination of thermal, plasma, and photochemical (electronic) processes [1]. For metals, thermal and plasma processes dominate in the range about 1 GW/cm^2, and evaluating these is basic to gaining a quantitative understanding of the vaporization process [2]. Two of the primary experimental quantities [3] to be interpreted are the amount of material removed and the degree of ionization within the plume. The present goals in this area are not only to measure them, but to determine these quantities from a model having the minimum number of assumptions, in order to more effectively identify the primary underlying phenomena [4]. The model [5] used in this study is based primarily on thermal (vapor pressure and diffusivity) data plus cross sections intrinsic to the inverse bremsstrahlung heating [6] of an electron cloud; it does *not contain adjustable parameters.*

The thermal data include the thermal diffusivity and the vapor pressure of the metal. The rate of vaporization is determined by maintaining the equilibrium vapor density

just above the Cu surface; expansion away from the surface is the result of the pressure gradients. For ease of calculation, the model is one-dimensional, since the diameter of a typical laser spot is ~1 mm^2, while the primary vapor interactions are frozen in at a much smaller height of ~0.2 mm. This simplification has a negligible effect *except* for micro focused equipment, e.g., LIMMA (laser-induced microanalytic mass analysis) probing.

The transition from simple thermal vaporization to plasma-controlled vaporization is dependent on the amount of laser beam energy deposited into the "free" electrons in the plume. The term "free" is qualified because the inelastic scattering of these electrons (known as inverse bremsstrahlung, IB) adds an imaginary (loss) component to their polarization when oscillating under the field of the incoming excimer laser beam. Furthermore, since the Debye shielding distance layer occupies only the outer shell of the plume, the dominant plasma behavior follows ambipolar diffusion of the plasma, implying negligible separation of ion and electron charge clouds. The inelastic scattering of the electrons is due either to their colliding with atoms or to coulombic scattering by ions [6]. The cross section of the latter process is one to two orders of magnitude larger than that of the former; however, only at the higher power levels ($I \gtrsim 500$ MW/cm^2) is the ion density sufficient to be the origin of the primary inelastic electron scattering [7]. Thus, the initial electron heating, either at low powers or early in the ~10-ns pulse, depends on the high *atom* (vapor) density.

The above inferences have been incorporated into a previously described model [5] that was used in this study. The model is relatively straightforward. It *assumes local thermodynamic equilibrium* (*LTE*), and includes IB in addition to the previously mentioned thermal diffusion in the solid, and vapor pressure of the solid or liquid surface.

The objective of the study described here was to compare the results of such modeling to laser-induced fluorescence (LIF) measurements above laser-ablated copper. Primarily the goal was to highlight the dominant features of the nanosecond transition from the solid to vapor and sometimes plasma state.

Identification of the dominant interactions and energy balances is a necessary step in understanding laser ablation for the deposition of high-critical-temperature superconductors or copper [8, 9]. Some of the questions that were viewed with an aim to understanding dominant mechanisms were the following: 1) Do the intensities and densities justify the LTE assumption? 2) Should the high degree of ionization be viewed as a thermal arc rather than a gas breakdown (even though the onset is rather sudden on an energy scale)? 3) Is the IB from neutrals sufficient to explain the original energy input? 4) Does adiabatic cooling [10] reduce the ionization, or does the plume density rapidly decrease to such a low value that the state of ionization is "frozen in"? Lastly, the present comparisons are useful in connection with analytic models [11] in the adjacent but slightly higher irradiance range ($\gtrsim 1$ GW/cm^2), where it is well known that the above-mentioned surface plasma dominates. While more complicated models [4] certainly exist, they are not universally available or transparent, particularly with respect to identifying the dominant effects. Also, the more elaborate models often contain assumptions that may be outside their range of validity, so less subtlety sometimes serves to verify and elucidate complicated multidimensional computer calculations.

The model

As mentioned before, central features of the model used were the assumptions of LTE and IB controlling the distribution of laser beam energy. Beyond that, primarily physical quantities characteristic of copper (e.g., ionization energies, vapor pressure, and the solid-state thermal diffusivity) were inserted. Note that this means there were *no adjustable parameters* in the analysis.

The LTE assumption appeared justified because many of the energy transfers occur at densities $\gtrsim 10^{19}$ cm^{-3}. At such values, three-body recombination and electron–atom energy transfer have nanosecond time constants [6, 7]. Also, at these densities the electron scattering frequency, $\gtrsim 5 \times 10^{12}$ s^{-1}, causes significant IB heating of the electron cloud [7]. This applies despite the fact that the laser frequency, $\omega/2\pi$, is far higher than the plasma cut-off frequency, $\omega_p/2\pi$. This relationship, however, is the origin of the $(\omega_p/\omega)^2$ roll-off in absorption as the wavelength approaches the ultraviolet range.

Depending on the governing energy deposition and redistribution processes, several phases of laser–solid interaction can be distinguished. During the *first phase*, the laser energy directly heats the copper surface. The heating rate and the surface temperature are defined by absorption and reflection coefficients, by thermal conductivity, and by the specific heat of the solid. In this phase the sole form of heat transport is conduction within the solid. The time development of axial temperature distribution $T(x, t)$ is described by the one-dimensional heat-conduction equation accounting only for transfer along the axis perpendicular to the target surface:

$$\frac{\partial T(x,t)}{\partial t} = \frac{\partial}{\partial x}\left[\left(\frac{K_s}{c_p^s \rho_s}\right)\frac{\partial T(x,t)}{\partial x}\right] + \frac{\alpha_s}{c_p^s \rho_s} I(t)(1 - R_s)\exp(-\alpha_s x), \quad (1)$$

where α_s, R_s, ρ_s, c_p^s, and K_s are the optical absorption and reflection coefficients, density, heat capacity, and thermal conductivity of the solid phase, respectively. The temporal

variation of laser irradiance during the pulse is denoted by $I(t)$.

The *second phase* of the interaction starts when the surface temperature reaches the melting point. At this stage two major changes occur: A melt front penetrates the solid phase, and the vapor pressure of molten copper exhibits exponential growth with temperature. The thermal and optical properties of the copper change during melting, resulting in significantly lower thermal conductivity and reflectivity. The heat conduction equation must be solved separately for the molten phase. It takes the form

$$\frac{\partial T(x,t)}{\partial t} = \frac{\partial}{\partial x}\left[\left(\frac{K_\ell}{c_p^\ell \rho}\right)\frac{\partial T(x,t)}{\partial x}\right] + \frac{\alpha_\ell}{c_p^\ell \rho} I(t)(1 - R_\ell)\exp(-\alpha_\ell x), \quad (2)$$

where the material parameters of Equation (1) are reindexed with ℓ subscripts or superscripts indicating the appropriate values for the liquid phase, and equivalently v for vapor later.

If the flux of particles j leaving the molten surface can be described by thermally activated surface vaporization, the process is governed by the surface temperature T_s. Thus,

$$j(T_s) = \frac{\beta p_0}{\sqrt{2\pi A R T_s}} \exp\left[\frac{\Delta H_{\ell v}(T_s - T_{\ell v})}{R T_s T_{\ell v}}\right], \quad (3)$$

where β denotes the sticking coefficient of surface atoms with atomic mass A. The terms $H_{\ell v}$, $T_{\ell v}$ are the enthalpy and temperature of the liquid–vapor phase transition at p_0 ambient pressure.

The enthalpy of fusion for copper, $H_{s\ell} = 13.0$ kJ/mol, is small compared to the enthalpy of vaporization, $H_{\ell v} = 304.8$ kJ/mol. Therefore, the energy loss due to melting was neglected in the calculations. The solid–liquid interface velocity can be calculated by tracing the $T(x, t) = T_{s\ell}$ point in the condensed phase temperature distribution. The liquid–vapor interface recession velocity, v_{surf}, can be expressed by the surface vaporization flux

$$v_{surf} = jA/\rho_\ell . \quad (4)$$

The presence of melt ejection under certain circumstances may become the dominating factor in surface recession. This possibility is excluded from the calculations.

Phase three starts when the plume density cannot be neglected and hydrodynamic expansion effects become relevant. The plume expansion is followed by assuming the following regarding the conservation of mass, momentum, and energy:

$$\frac{\partial \rho_v}{\partial t} = -\frac{\partial(\rho_v v)}{\partial x}, \quad (5)$$

$$\frac{\partial(\rho_v v)}{\partial t} = -\frac{\partial(p + \rho_v v^2)}{\partial x}, \quad (6)$$

$$\frac{\partial\left[\rho_v\left(e + \frac{v^2}{2}\right)\right]}{\partial t} = -\frac{\partial\left[\rho_v v\left(e + \frac{p}{\rho_v} + \frac{v^2}{2}\right)\right]}{\partial x} + \alpha_v I_0(t)\exp(-\alpha_v x) - \varepsilon_{rad}, \quad (7)$$

where ρ, ρ_v, c, v, p, and α_v denote the density, internal energy density, hydrodynamic velocity, pressure, and light absorption coefficient of the vapor, respectively. The ε_{rad} power loss is calculated assuming only bremsstrahlung radiation. The α_v absorption coefficient has two components: the electron–neutral and the electron–ion inverse bremsstrahlung contributions. Before the vapor effectively breaks down, the absorption process is dominated by the electron–neutral interaction. If the laser fluence is above the plume threshold, a rapid increase in ion density tips the balance in favor of electron–ion interactions (as discussed in the next section). This is the beginning of an optional fourth phase in the interaction, in which the vapor phase is completely ionized and nearly completely absorbs the incoming laser light. Ion generation in the model is treated as the consequence of thermionic emission from the heated surface and as thermal ionization in the vapor. These processes are described by the Langmuir–Saha and Saha–Eggert equations [6], respectively.

The temporal characteristics of the laser are studied using two different pulse shapes. For most of the calculations, the so-called "top hat" approximation is applied:

$$I_0(t) = \begin{cases} I_0 & \text{if } 0 < t < \tau_{pulse} \equiv \tau, \\ 0 & \text{otherwise,} \end{cases} \quad (8)$$

where τ_{pulse} is the effective length of the laser pulse. Additional trials are made using a stepwise decaying pulse shape representing the same $I_0\tau$ pulse fluence, viz.,

$$I(t) = \begin{cases} 2I_0 & \text{if } 0 < t < \tau_{pulse}/4, \\ I_0 & \text{if } \tau_{pulse}/4 < t < \tau_{pulse}/2, \\ I_0/2 & \text{if } \tau_{pulse}/2 < t < \tau_{pulse}, \\ 0 & \text{otherwise.} \end{cases} \quad (9)$$

This profile seems to be a better representation of the XeF excimer laser pulse than that of Equation (8).

We must emphasize that the four phases of the model cannot be separated in time because of substantial overlap between some of them. Therefore, all equations must be solved simultaneously, and the solutions for the vapor, liquid, and solid regions must satisfy coupling boundary conditions. This is a significant departure from many of the

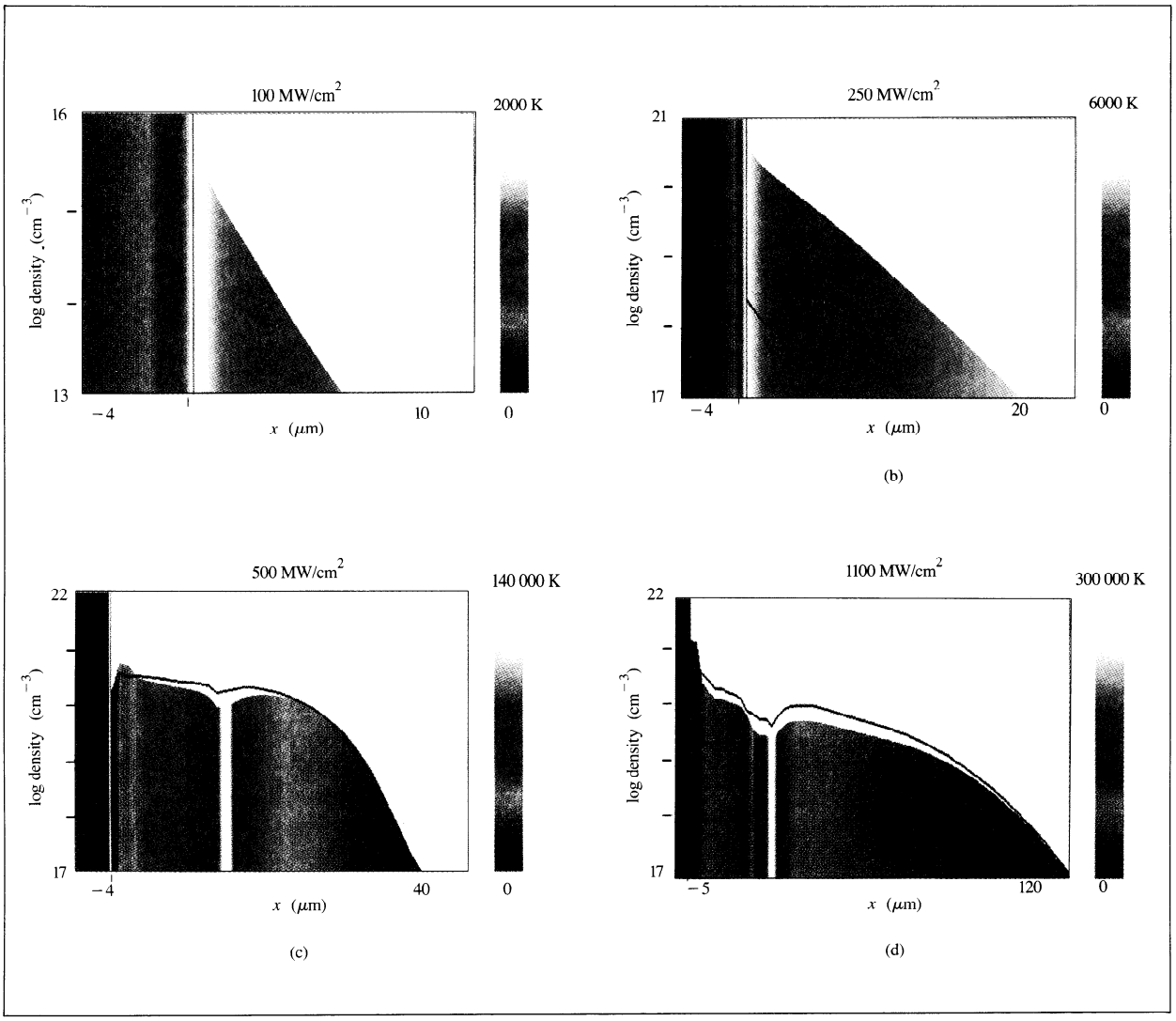

Figure 1

Modeling of the Cu vapor density and temperature (color scale) as a function of distance from a Cu surface being ablated by means of a 351-nm excimer laser. The images represent the plume characteristics at the end of the 10-ns laser pulse. The laser beam is presumed to impinge from the right. Note that the total Cu density (top of the colored area) is depicted by a logarithmic scale covering several orders of magnitude. The free electron density is shown as a black line, which lies above the Cu density level when double ionization is dominant. The original solid surface is shown as a vertical line; the negative x-dimension refers to the subsurface depth of the display. (a) At a low irradiance (100 MW/cm^2), where the vaporization is purely thermal and the ionization is completely negligible: The maximum temperature at the *end* of the 10-ns pulse is 1850 K, and heat has diffused down into nearly 1 μm of metal. This relatively low temperature produces a Cu vapor density of only 3×10^{15} cm^{-3} and little $p \cdot V$ driving energy to accelerate the vapor ejection. (b) At an irradiance of 250 MW/cm^2: Note that now the ionization is ~0.5% and the surface temperature is 5000 K. Plume absorption has not yet begun; hence, the temperature rise is approximately proportional to irradiance, following (a). The ionization is due to the elevated surface temperature as it continues for a few nanoseconds after the laser pulse ends at 10 ns. (c) At an irradiance of 500 MW/cm^2: The maximum surface temperature is 7200 K but is reached in 6 ns as a result of the occurrence of some cooling (to 6600 K) due to the presence of the free electrons in the plume. These free electrons have sufficient optical absorption cross section (IB) and density to attenuate the last few nanoseconds of the excimer beam (i.e., shadowing). In return, the plume temperature is elevated by the additional laser beam absorption, IB, to over 10^4 K. The result of this additional heating is an ~100% ionized plume, except for the material just leaving the surface at 10 ns. In this latter case, only the thermal ionization (~0.5%) is present; nevertheless, the vapor density remains at $>10^{20}$ cm^{-3}. Also, the fact that IB requires significant density of scattering centers to avalanche is evident, since in the other extreme the low-density leading edge of the expanding vapor is virtually unheated. (d) At an irradiance of 1.1 GW/cm^2: This fluence level results in major plume absorption, with resulting temperatures $>3 \times 10^5$ K, corresponding to an energy of 27 eV. Such an energy is obviously sufficient to doubly ionize copper; hence, the electron density is about twice the Cu density in the plume, but the surface temperature maximum is about 7200 K at $t \sim 2$ ns. The final surface temperature (at 10 ns) is about 5500 K, thus showing even stronger shadowing than in (c). The ever-increasing inflections in the density near 25 μm may indicate an instability beginning to grow into a discontinuity characteristic of a shock wave.

previous models, in which the individual stages were handled independently.

The excimer laser etching pulses are represented as flat-topped 10-ns pulses. The results obtained in this study were depicted as a series of figures spaced at 1-ns intervals; specific examples at $t = 10$ ns are shown in **Figure 1**, i.e., at the turn-off point of the laser pulse. As mentioned above, runs were also carried out using a pseudo-exponential decaying intensity; the latter closely approximates an excimer laser pulse. (Slightly lower temperatures and densities with a pseudo-exponential profile were due to the fact that the beam energy was dissipated over a greater depth because of the extended time for downward thermal diffusion of several nanoseconds before the maximum vapor pressure was reached.) Furthermore, only the diminished (weak) late laser beam was then producing the IB. For a given fluence, these decaying pulses gave reduced IB, as would be expected from the above. The differences, however, were not dramatic (<50% decrease in densities), while lacking the illustrative capability of the flat-top pulses, particularly with respect to showing the onset of plume shadowing of the incoming excimer beam.

Some of the primary points that may be noted in the figures are the following: The maximum temperature at 100 MW/cm^2 is 1850 K and is reached at 10 ns. No ionization (<10^{-5}%) is noted, since the maximum vapor density is only ~3×10^{15} cm^{-3}; hence, the inelastic scattering of electrons leading to IB is completely negligible. The data indicate that about 10^{11} Cu atoms/cm^2 are removed (i.e., ~10^{-4} monolayers). The heat penetrates about 0.5 μm into the solid, a distance which is essentially constant over all energies, since it is essentially a function of only the pulse length and thermal diffusivity. At 250 MW/cm^2 several new features become apparent. The Cu density near the surface escalates to ~10^{20} cm^{-3}, and the expansion velocity increases to >10^5 cm/s. The fractional ionization is at ~0.5% and is due to thermal ionization. This is evidenced by the fact that the ion fraction remains constant even in the vapor leaving the surface immediately after the end of the 10-ns laser pulse [see Figure 1(b)]. The surface temperature is ~5000 K, which is in agreement with the increased fluence and additional heating with liquid Cu surfaces.

At 500 MW/cm^2 the ionization increases to essentially 100% because of *vapor cloud* heating into the 1.5×10^5 K = 13 eV region, even though the surface remains near 6000 K. The temperature maximum is at about 6 ns and shows the onset of plume absorption, i.e., shadowing of the surface during the last 4 ns of the laser pulse. This sequence of surface temperatures is depicted in **Figure 2**, where it is seen that T increases monotonically upward at 250 MW/cm^2. However, at both 500 MW/cm^2 and 1.1 GW/cm^2 a maximum appears *before* the end of the laser pulse.

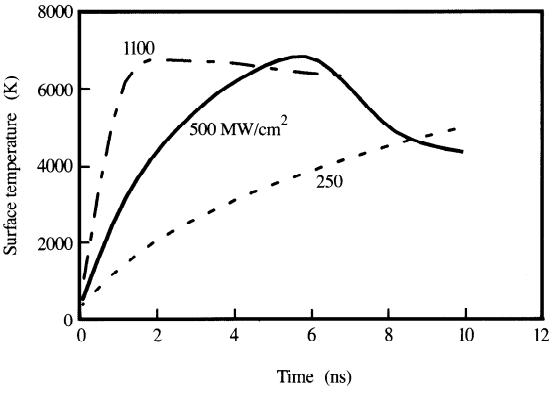

Figure 2

Calculated surface temperature T_s as a function of time during a 10-ns pulse. Note that the (above surface) plasma becoming opaque is evidenced by surface cooling before the completion of the 0.5- and 1.1-GW/cm^2 pulses. On the other hand, the 250-MW/cm^2 pulse does not avalanche within the 10-ns pulse, thus avoiding surface shadowing.

At 1.1 GW/cm^2 the IB is so intense that the ionization produces Cu^{++} over a fraction of the plume, as indicated by the electron density being greater than the total copper density. Also, it is noted that T_s is essentially constant at a value near 6800 K, indicative of strong shadowing. The electron cloud becomes sufficiently opaque that only a minor fraction of the laser beam in its later stage can penetrate to the surface. These three higher-power levels illustrate why the plasma formation appears similar to an arc; e.g., some ionization is always present, but additional energy input causes an exponential avalanche in (vapor-phase) thermal ionization. Nevertheless, the vapor state has now transformed from a low level of ionization to complete ionization and finally to surface shadowing, with each transition requiring at most a 2:1 increase in irradiance and giving an outward appearance of a sudden onset of the plasma state.

Comparison of the modeling to LIF results

Figure 3 compares the model to LIF results [3] for Cu^0 atoms. Note that the *data cover five decades* in Cu^0 yield and a 2:1 fluence range; nevertheless, the slopes are equal. However, the lower yield from the modeling suggests that the material removal corresponds to an ~20% higher fluence than obtained by means of surface profile and LIF measurements. Two features appear to underlie this difference: First, even apertured excimer beams are not perfectly uniform, but contain "hot" and "cold" areas.

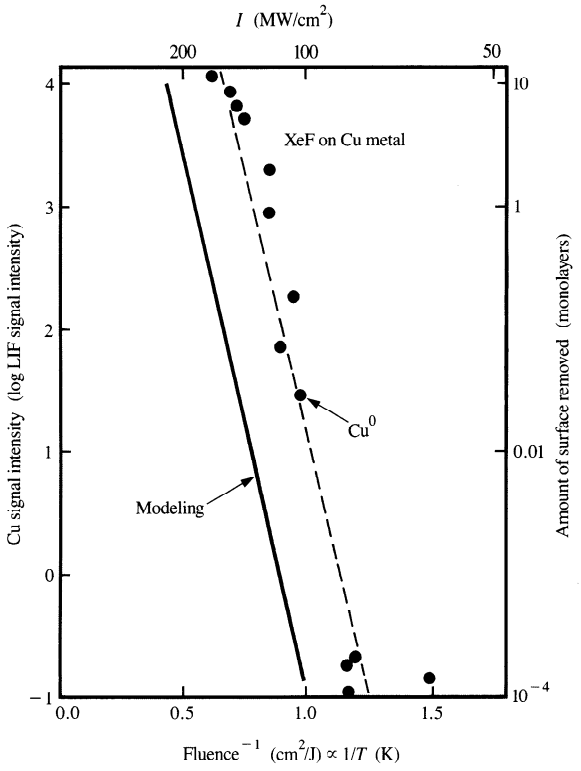

Figure 3

Comparison of the present modeling result (solid line) to the LIF result of [3]. The LIF yield was previously normalized at the 10-monolayer point by a surface profile measurement. This value, near the maximum of the removal range of this material, thereby permits the *relative* LIF results to be put on an absolute scale.

The "hot" areas dominate the vaporization because of the strongly exponential dependence of vapor pressure on temperature. Second, *molten* surfaces (at a depth of ~0.25 μm in this study) may support wavelets which enhance the laser absorption due to the rough surface texture [12]. Taken together, it is not surprising that a 20% difference in fluence is found for the predicted and observed etch rates.

Figure 4 shows the dependence of the intensities of Cu^0 and metastable Cu^+ ion signals as a function of fluence. A primary point of the previous result [3] is the decrease of the Cu^0 signal and rapid elevation of that of the Cu^+ for $F > 3$ J/cm^2; i.e., $I > 300$ MW/cm^2. This is precisely the fluence range in which the present calculated ionization rises rapidly from <1% to ~100%. Thus, the viewpoint that IB is extracting laser energy by plasma electrons scattering first from neutrals and subsequently from the resulting ions appears valid. The rapidity of the onset with irradiance appears due to the strong dependence of the vapor density on fluence; i.e., the exponential vapor pressure simulates a slope equivalent to a highly multiphoton dependence. Finally, once the ion density has increased perceptibly (exponential in T) as a result of heating, the dephasing electron collisions escalate because of (long-range) coulombic scattering.

At low fluences (1 to 2 J/cm^2), the value of the LIF signal from the Cu^+ ions indicates that the origin of these Cu^+ ions is true multiphoton ionization. As is evident from the $(\omega_p/\omega)^2$ roll-off, 351-nm radiation would have been nearly twice as effective as 193-nm in producing electron heating by IB; by comparison, the LIF signal from the Cu^+ ions compared to that from the Cu^0 ions has approximately an I^3 dependence at 351 nm, while it has an I^1 dependence at 193 nm [3]. The modeling indicates that the temperature of the copper is insufficient to generate significant Cu^+ ions by a thermal mechanism at $F \lesssim 2$ J/cm^2. Also supporting this interpretation is the fact that thermal ions display a very steep dependence on irradiance, as typified by the lower dashed line in Figure 4. It thus appears that in the experimental behavior the surface-emitted ions (F = 2–3 J/cm^2) are merged into the surrounding multiphoton ionization and thermal ionization in the vapor (because of intense IB at the higher fluences). The strength of multiphoton ionization is presumably aided by two features: 1) high temperatures (>2000 K), thus eliminating a second photon requirement in the 193-nm effects, and 2) nearby intermediate states for Cu ($\lesssim$2000 cm^{-1}), thus enhancing the transition probability.

Multiphoton and thermally generated free electrons facilitate the achievement of equilibria by providing the seed electrons for further avalanche ionization. This is in contrast to the breakdown behavior with noble gases, in which multiphoton ionization is a rarity and often restricts the electron avalanche. In this latter case, however, the medium is a very pure, dust-free noble gas [13]. Note that this contrasts with the present case, in which clusters, particulates, etc. are generated in the nanosecond transition from solid to vapor, causing the initial step to be effectively bypassed.

One question that might be asked is "How is local thermodynamic equilibrium achieved?" As we have just seen with noble gases, a state of nonequilibrium is in effect that must await the first few free electrons before avalanching into an equilibrium plasma state. In the case of Cu ablation, free electrons are always present. Since their density is small, coupling their energy into the entire Cu^0 density is not rapid via three-body recombination. One reason is that the relaxation time τ_{e0} (for electron energy loss) is about 2 ns; hence, energy can barely be transferred, and then only for heating near the first half of the excimer pulse; insufficient time is available during the important last 2 ns of the excimer pulse because of the low density of Cu away from the surface. Hence, a finite

number of "hot electrons" should exist which are capable of avalanching the ionization. Another reason is that it is reasonable to presume the presence of local hot spots (excimer beams are *not* single mode), and high Cu densities which will avalanche small volumes into a highly ionized state. These local volumes should propagate rapidly [13] into the surrounding volume because of their enhanced scattering by long-range coulombic forces and free-electron diffusion into the surrounding media. This tendency to achieve LTE makes the laser surface interaction under study resemble a (high-temperature) thermal arc rather than paralleling the spark-like breakdown of noble gases.

The temperatures for $I \geq 500$ MW/cm^2 nearly completely dissociate the fraction of the vapor that evaporates as Cu_2 diatomic. As illustrated in Figure 1, the difference in surface temperature between irradiances of 250 and 500 MW/cm^2 is not significant; both result in a temperature of ~5000 K. On the other hand, the latter irradiance raises the *plume* temperature to 1.5×10^5 K and hence readily dissociates the Cu_2. It appears that little Cu_2 is stable in the high-temperature portion of the plume. Only Cu_2 in the low-temperature, last-vaporized material should be stable, i.e., the volume near 1 μm in Figure 1(c). It should be possible to evaluate the fraction of Cu_2 remaining by integrating over the various $T(x)$ values. Note, however, that the view of survival of *late* Cu_2 is supported by the observation that diatomics *appear* to slow down concurrently with their dissociation [14, 15].

The Boltzmann velocity of Cu^0, modeled at an irradiance of 500 MW/cm^2, is 0.55 cm/μs and increases to 0.7 cm/μs at 1.1 GW/cm^2. These values approach the analytical model of Phipps et al. [11], which predicts 0.72 cm/μs and 0.88 cm/μs, respectively. Both these velocities are ~50% below the experimental values; however, the coulombic forces which accelerate ions have not been included [10]. At lower irradiance levels the calculated velocities are low, primarily because the initial velocity of recoil ($kT \sim 0.4$ eV ~ 0.11 cm/μs) from the surface that is related to effusive thermal vaporization was not included in the modeling.

Conclusions

Analyses based on a previously described model utilizing LTE and IB (with scattering due to both atoms and ions) and containing no adjustable parameters explain most of the features of the thermal-to-plasma etching transition for Cu. Most significantly, the transition appears at the correct power density. Radiative and adiabatic cooling are present but not dominant. The main features explained by the model are the amount of Cu removed and the breakdown (ionization) avalanche.

The thermal conductivity of the plasma has not been incorporated into the analyses. Whether or not such

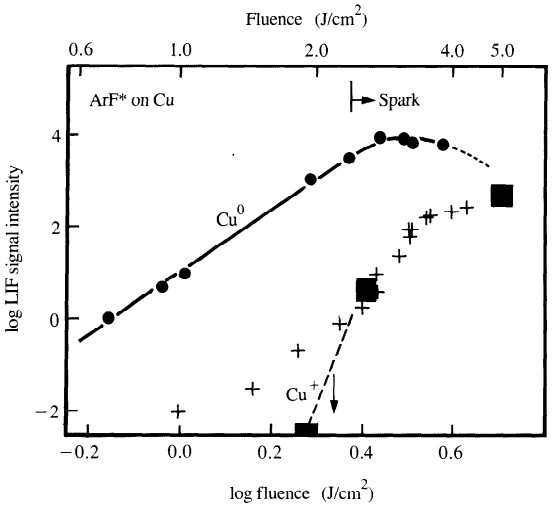

Figure 4

The LIF signal from Cu^0 and Cu^+. The Cu^+ was detected in a metastable state (up 1 eV) [3]. Probe measurements indicated that the ground-state Cu^+ is ten times more dense than the metastable state; this ratio has been incorporated in translating the modeling results into the calculated Cu^+ densities, depicted as squares.

processes are included is not a primary concern, since it has been shown [11] that approximately e^{-1} of the energy *must* reach the surface by *some* mechanism in order to provide the requisite vaporization rate. Without this vaporization rate the free electron scattering and IB would diminish and the surface would automatically receive additional energy. As a consequence, the plasma shadowing can be looked upon as furnishing a negative feedback type of control. In the far infrared (CO_2 laser) range, the feedback becomes so strong (and shifted in phase) that the system can break into cyclic oscillations [2].

In the modeling described, cooling is somewhat overestimated because the molecular motion is frozen at a Cu vapor density of ~10^{16} cm^{-3} [Figure 1(c)]; this occurs because of the sparsity of collisions (in <1 μs) at lower densities.

Evidence of plume absorption appears in the calculated temperatures, as would be expected from the IB *above* the surface. The modeling results connect smoothly with the analytical expressions of [10] and [11] and with modeling of similar systems [16]. This is to be anticipated, since in the above references the plume absorption is simply inserted as an e^{-1} beam attenuation, a value which approximates the asymptote obtained in this study.

In summary, the analyses described here accurately characterize the major features of copper ablation and plasma formation. The model used should therefore be

helpful for gaining insights regarding reactions such as the reoxidation of Cu during the deposition of high-critical-temperature superconductors.

Acknowledgments

A. Vertes acknowledges the support of the NSF (Grant No. CTS-9212389) and the George Washington University Facilitating Fund. The authors also wish to acknowledge helpful discussions with C. Phipps of Los Alamos National Laboratory and E. Matthias of the Free University of Berlin, as facilitated by NATO Research Grant No. SA.5-2-05(CRG.880020)1133/90AHJ-514.

References and note

1. R. W. Dreyfus, *Laser Ablation of Electronic Materials: Basic Mechanisms and Applications*, E. Fogarassy, Ed., Elsevier Publishers, London, 1992, p. 61.
2. J. F. Ready, *Effects of High-Power Laser Radiation*, Academic Press, Inc., Orlando, FL, 1971; R. E. Kidder, *Proc. Internat. School Phys.*, No. 48, P. Caldirola and H. Knoepfel, Eds., Academic Press, Inc., New York, 1971, p. 306.
3. R. W. Dreyfus, *J. Appl. Phys.* **69**, 1721 (1991).
4. G. Zimmermann and W. Kruer, *Comments Plasma Phys.* **2**, 51 (1975).
5. A. Vertes, P. Juhasz, M. De Wolf, and R. Gijbels, *Scanning Microsc.* **2**, 1853 (1988); *J. Mass Spectrosc. & Ion Process.* **94**, 63 (1989) and references therein.
6. Inverse bremsstrahlung is the absorption of laser energy by "free" electrons due to their inelastic scattering primarily by ions. See D. L. Book, *AIP 50th Anniv. Phys. Vade Mecum*, H. Anderson, Ed., American Institute of Physics, New York, 1989, p. 278; T. W. Johnston and J. M. Dawson, *Phys. Fluids* **16**, 722 (1973).
7. R. W. Dreyfus, *Surface Science*, Profs. K. Terakura and Y. Murata, Elsevier/North-Holland, Amsterdam, 1993, p. 177.
8. C. E. Otis and R. W. Dreyfus, *Phys. Rev. Lett.* **67**, 2102 (1991).
9. B. Braren, A. Sugerman, and F. Turene, *Post-Deadline Paper CPDP 35*, Conference on Lasers and Electro-Optics, Baltimore, MD, May 12–17, 1991.
10. C. R. Phipps and R. W. Dreyfus, "Laser Ablation and Plasma Formation," book chapter in *Laser Ionization Mass Analysis*, A. Vertes, R. Gijbels, and F. Adams, Eds., John Wiley & Sons Publishers, New York, 1993, p. 369.
11. C. R. Phipps, T. P. Turner, R. F. Harrison, G. W. York, W. Z. Ozborne, G. K. Anderson, X. F. Corlis, L. C. Haynes, H. S. Steele, and K. C. Spicochi, *J. Appl. Phys.* **64**, 1083 (1988) and references therein.
12. A. Annino, F. Grasso, F. Musumeci, and A. Triglia, *Appl. Phys. A* **35**, 115 (1984).
13. C. Grey Morgan, *Rep. Prog. Phys.* **38**, 621 (1975); A. Alcock, *Laser Interactions and Related Plasma Phenomena*, Vol. II, H. Schwartz and H. Hora, Eds., Plenum Publishing Co., New York, 1972.
14. R. W. Dreyfus, Roger Kelly, R. E. Walkup, and R. Srinivasan, *Proc. SPIE* **710**, 46 (1986).
15. D. Pappas, J. Cuomo, K. Saenger, and R. W. Dreyfus, *J. Appl. Phys.* **72**, 3966 (1992).
16. L. Balazs, R. Gijbels, and A. Vertes, *Anal. Chem.* **63**, 314 (1991).

Received November 20, 1992; accepted for publication September 28, 1993

Akos Vertes *Department of Chemistry, The George Washington University, Washington, DC 20052 (vertes@gwuvm).* Dr. Vertes received a B.S. degree in chemistry in 1974 at the Eotvos Lorand University, Budapest, Hungary, and a Ph.D. in chemistry in 1979 at the same university. From 1979 to 1990 he worked at the Central Research Institute for Physics of the Hungarian Academy of Sciences, first as a Research Associate and later as a Senior Research Associate. From 1987 to 1990, he also served as Deputy Head of the Chemistry Department. From 1987 to 1991, he held the position of Associate Professor at the University of Antwerp, Belgium. Since 1991, he has been an Associate Professor of Chemistry at The George Washington University. His research interests encompass the application of lasers and other plasma ionization sources in mass spectrometry. His theoretical modeling work includes the description of laser–solid interactions and plasma ionization sources in general. Dr. Vertes is a member of the American Chemical Society and the American Society for Mass Spectrometry.

Russell W. Dreyfus *Faculté des Sciences de Luminy, Département de Physique, Case 901 (Groupe des Etats Condensés), Université d'Aix-Marseille II, 13288 Marseille Cedex 9, France (dreyfus@gpec.univ-mrs.fr).* Dr. Dreyfus retired from IBM in 1993. He was a Research Staff Member investigating the laser ablation of solids in the Physical and Inorganic Chemistry of Surfaces group within the Chemistry and Material Sciences Department. He is currently an Associate Professor in the Condensed State Physics Group of the University of Aix-Marseille. Prior to retiring from IBM, he used laser-induced fluorescence techniques to study the physical and chemical processes produced by vaporization with nanosecond ultraviolet laser pulses. Dr. Dreyfus received his B.S. and M.S. degrees from Purdue University in 1951 and 1953, respectively. He began working at the IBM Research Division in 1958 and concurrently completed his Ph.D. at Yale University in 1960. During his time at IBM, he worked in the areas of ultraviolet and VUV lasers, spectroscopy, solid-state physics, ultrasonics, and high-speed photography. Dr. Dreyfus has published over 90 scientific papers and holds 17 U.S. patents. He is a Fellow of the American Optical Society and the American Physical Society.

Daniel E. Platt *IBM Research Division, Thomas J. Watson Research Center, P.O. Box 218, Yorktown Heights, New York 10598 (PLATT at WATSON, platt@watson.ibm.com).* Dr. Platt received a Ph.D. in physics from Emory University in Atlanta. He joined IBM at the Thomas J. Watson Research Center in 1989 as a Research Staff Member. His areas of research have included diffusion-limited growth, deposition, percolation, Monte Carlo simulation of thermal processes, scientific visualization, and, recently, the development of routines for commercial video production by commercial film-making companies.

Presented To

Akos Vertes

In Appreciation For
Publishing The Article

Modeling the thermal-to-plasma transitions for Cu photoablation

In The *IBM Journal*
of Research and Development

Editor